



Proton-Induced Microchemical and Microstructural Changes in Austenitic Stainless Steels

Takuji Fukuda¹⁾, Yoshihiro Isobe¹⁾, Akira Hasegawa²⁾, Manabu Sato²⁾ and Katsunori Abe²⁾

1) Nuclear Fuel Industries, Ltd., Japan

2) Tohoku University, Japan

ABSTRACT

In austenitic steels used for light water reactors, neutron irradiation induced the microchemical and microstructural changes in matrices and around grain boundaries, which are related to various property changes, such as irradiation hardening and irradiation assisted stress corrosion cracking (IASCC).

The grain boundary segregation and the microstructural development depend on irradiation conditions, such as dpa levels, helium contents and temperatures etc. The effects of helium, however, have not yet been clarified. This paper presents microchemical and microstructural changes in SUS304, SUS347, SUS310, and XM-19 stainless steels implanted with helium and irradiated with proton. The irradiation tests were carried out using Dyanimitron accelerator at Tohoku University.

1.INTRODUCTION

According to past literature regarding irradiation damage for austenitic steel under fast reactor conditions, mobility of point defects such as interstitial and vacancy increases at higher temperatures, which results in suppressing recombination of the defects. Accordingly, irradiation damage basically increases with increasing irradiation temperature. On the other hand, since mobility of the defects decreases under low temperature, irradiation induced degradation seems to be not so active under 400°C. However, phenomena of the degradation under 400°C have not been clarified. This study was therefore focused on microchemical and microstructural changes of several austenitic steels irradiated 300°C.

2.EXPERIMENTAL PROCEDURE

Table 1 shows the chemical composition of the specimens. Specimens prepared from SUS304, SUS347, SUS310 and XM19. Cold rolled steels of 0.25mm thickness were solution annealed at 1000°C for 5 minutes. The grain size of these steel sheets were controlled to be under 10 μm. Irradiation specimens were electropolished to 0.15mm thickness to remove the surface oxide layer and punched out into disks 3mm in diameter.

Irradiation was carried out using 3 MeV He⁺ ion with energy degrader at room temperature, which simulates the effect of He generation via Ni two-step sequential reaction

in core materials ($^{58}\text{Ni}(n,\gamma)^{59}\text{Ni}(n,\alpha)^{56}\text{Fe}$)¹ and 2 MeV H_2^+ ion at 300°C to produced displacement damage to 1dpa. He were injected prior to H_2^+ ion irradiation which are reported to correspond to the amount of He generation from Ni (n,α) reaction of about 1 cycle in PWR power plant about $1.2 \times 10^{21} \text{n/cm}^2$ and life terminal of some core internals in LWR². The depth distributions of pre-injected He atom concentrations and displacement damage were estimated using TRIM code (Fig.1). During H_2^+ irradiation, target temperature was controlled to be $300 \pm 5^\circ\text{C}$ through beam heating and a heat panel placed at backside of the disk, and monitored by infrared pyrometer. Irradiation beam was collimated to be 3 mm in diameter. The energy degrader was used to make the distribution of injected He concentration uniform at depth ranging from 1.5 to 3.5 μm. The irradiation tests were carried out using Dynamitron accelerator at Tohoku University.

After the irradiation, samples were not radio activated. The test samples were thinned by electro-chemical polishing from irradiated side and back side. Chemical compositions at grain boundary and microstructure were examined using FE-TEM (field emission-gun transmission electron microscope HITACHI HF-2000) and energy dispersive spectroscopy (EDS). Analyzed elements were Fe, Ni, Cr, Si, P, Mn and Mo. The thickness of TEM observed area was evaluated by electron energy loss spectroscopy (EELS). Quantitative analysis of the chemical composition was performed with a probe less than 1 nm diameter.

Micro-indentation test was conducted for both as-irradiated and unirradiated irradiation XM-19 samples to detect irradiation induced changes in mechanical properties.

3.RESULTS

3.1 Grain Boundary Segregation

No precipitate of chromium carbides occurred at grain boundary in unirradiated samples. The concentrations of alloy elements near grain boundary are summarized in Table 2. Drastic changes in alloy compositions were observed within 5 nm areas from grain boundary in each irradiated sample (Fig.2). Si and P were increased at grain boundary for all irradiated samples. Mn and Mo were decreased at grain boundary for irradiated XM-19.

In the Table 2 segregation ratio is defined as

$$(\text{Cr af} - \text{Cr bf}) / \text{Cr bf} \times 100 \quad (\text{Eq.1}),$$

where Cr bf and Cr af are Cr concentrations at grain boundary before and after irradiation, respectively.

3.2 Microstructural Observation

Results of TEM examination on microstructures and swelling were summarized in Table2, where swelling was measured by TEM observations. Swelling, Sw is expressed by

$$\text{Sw} = dV / (V_{\text{irr}} - dV) \quad (\text{Eq.2}),$$

where dV and V_{irr} are volumes of cavities and TEM observation region, respectively. Fig.3 shows the TEM observation results. Small cavities were observed in all irradiated samples except SUS304 without He pre-injection. The density of the cavity in SUS304 with 2000

appm He was higher than that in SUS304 with 15 appm He. Similarly, XM-19 steel with 2000 appm He showed higher density of the cavity than that with 15 appm He. The average diameter of the cavity seen in XM-19 steel with 15 appm He was largest in this study. The average cavity size decreased with increasing the amount of pre-injected He. Swelling decreased with increasing of pre-injected He concentration in XM-19, however this trend was not found in SUS 304.

To clarify the effect of He pre-injection, samples irradiated only by H_2^+ were prepared for SUS304 and XM-19 steels. Few cavities were recognized by TEM in XM-19 but no cavities were observed in SUS304.

3.3 Micro-Indentation Test

Fig.4 illustrates the result of micro-indentation test for XM-19 with 15 appm He, showing irradiation hardening at surface layer. In the case of 5 gf-load, the hardness of irradiated sample was approximately 150 % higher than that of irradiated one.

4.DISCUSSION

4.1 Microchemical Change

4.1.1. Effect of chemical composition on RIS

Migration of alloy elements near grain boundaries results in RIS, which is caused by super-saturated defects, such as interstitial atom and vacancy sinking at grain boundary or surface. This phenomenon is explained by inverse Kirkendall effect or size effect of solute atoms. To evaluate the effect of bulk Ni and Cr concentrations on RIS, test results for irradiated alloys with 15 appm He were compared. The result indicates that increasing bulk Ni and Cr concentrations enhanced the amount of segregation. Similar trends appeared in past studies^{5,6}. Some studies reported that these phenomena were suppressed when over-sized atoms were contained in irradiated materials^{3,4}. Thus in order to evaluate the behavior of over-sized element except Cr, SUS347 and SUS310 were chosen as samples containing oversized atom compared to Fe atom, namely, Nb atom. XM-19 was also chosen in this study as a test alloy containing over-sized Mn atom. The result shows that there was no effect on suppressing Cr segregation by adding over-sized atom in XM-19 and SUS310 steels. However in SUS 347 suppression of Cr segregation was observed.

4.1.2 Effect of irradiation particle on RIS

The present results of RIS induced by He^+ and H_2^+ ion irradiations corresponded to RIS induced by neutron irradiation qualitatively. However, the extent of RIS produced by He^+ and H_2^+ ion irradiation was nearly ten times larger than that produced by neutron irradiation, SUS304 even at the same dpa⁷. The formation efficiency of freely migrating defect (fmd), which controls the diffusivity of the solute atom, was reported to be ten times higher with proton irradiation than with neutron irradiation⁸. Considering this difference in formation efficiency of fmd, the amount of RIS in this study seems to correspond quantitatively to that by neutron irradiation [7].

4.2. Microstructural Change

No cavity was observed in XM-19 steels pre-injected only by He to 15 appm in our past experience. However, as shown in Fig 3, cavities were observed in samples irradiated by

H_2^+ or He^+ plus H_2^+ ions except SUS304 sample without He pre-injection. Hence, observed cavities were related to displacement damage and accumulation of helium and hydrogen in the sample. According to past studies^{10,11} reporting the effect of pre-injected or simultaneously injected helium behavior in materials, density of voids tended to increase and diameter of voids tended to decrease compared with no helium pre-injection. This suggests that pre-injected helium decreases the energy of void nucleation and causes higher void density. In XM-19 and SUS304 samples with 2000 appm helium had larger cavity density compared to the samples with 15 appm helium. (Fig.6) These results showed good agreement with past studies.

By irradiation only by proton some cavities were observed in XM-19 but no cavity in SUS304 sample. These results showed that formation of cavity was mainly caused by irradiation of H_2^+ but nucleation was affected by pre-injected helium. The microstructural observation of SUS304, SUS347 and SUS310 suggested that addition of Nb may suppressed swelling. This is because the sink effect at the boundary between NbC and the matrix. TEM observation indicated many NbC in the matrix grain of SUS347 and SUS310.

4.3 Mechanical Properties Changes

Results from micro indentation tests suggests that surface hardening occurred after irradiation. This may be due to microstructural changes such as higher density of dislocation and cavities introduced by irradiation. The results of micro-indentation testing with 5 gf-load shows remarkable difference compared with testing with 20 gf-load. This is because the result of 5 gf load was more affected by surface area hardening than that of 20 gf.

5.CONCLUSIONS

The following are conclusions.

- (1) Irradiation by 2 MeV H_2^+ at 300 °C to 1dpa induced depletion of Cr and enrichment of Ni at grain boundaries in SUS304, SUS347, SUS310 and XM-19 steels.
- (2) The amount of Ni and Cr segregations increased when Cr and Ni concentration .
- (3) Cavities were observed in all irradiated conditions except SUS304 without He pre-injection.
- (4) The cavity density increased and cavity size decreased when He contents increased in the samples, suggesting that helium played an important role for nucleation of the cavity.
- (5) Micro-indentation test test indicated that surface hardening occurred for irradiated samples.

REFERENCES

1. C.H.De Readt, Proc.Conf, on Fast, Thermal and Fusion Reactor Experiments.
2. F.A.Garner., et al. Proc. 6th Int. Symp. on Environmental Degradation of Materials in Nuclear Power Systems-Water Reactors, (1993) p783.
3. N.Shigenaka., et al.: J. Nucl. Sci. and Tech., Vol.33, No.7. 577(1996).
4. S.Kasahara., et al.: J. Nucl. Mater., Vol.239,194(1996).
5. D.L.Damcott., et al.: J. Nucl. Mater., Vol.225,97(1995).
6. H.Kinoshita., et al.: J. Nucl. Mater., Vol.239,205 (1996).
7. K.Asano, K.Fukuya, Proc. 5th Int. Symp. on Environmental Degradation of Materials in

- Nuclear Power Systems-Water Reactors, (1992) p838 The Metallurgical Society.
 8. G.S.Was, et al. Material Characterization Vol.32.239(1994)
 9.D.L.Damcott., et al. Mat. Res. Soc. Symp.Proc.Vol.373,131 (1995).
 10.Y. Katoh., et al. J. Nucl. Mater. 210,290(1994).
 11.Y.Murase., et al. J. Nucl. Sci. and Tech., Vol.33, No.3,239 (1996).

Table 1 Chemical composition of the sample alloy (wt%)

Alloy	C	Si	Mn	P	S	Ni	Cr	Mo	Nb	B	N	V	Fe
SUS304	0.06	0.57	1.12	0.032	0.007	8.66	18.20	-	-	-	-	-	Bal
SUS347	0.02	0.34	1.73	0.012	0.001	10.01	17.62	0.130	0.41	-	-	-	Bal
SUS310	0.01	0.24	0.68	0.008	0.004	20.42	25.49	-	0.18	-	-	-	Bal
XM19	0.03	0.45	4.85	0.016	0.001	11.90	21.90	2.160	0.20	-	0.31	0.19	Bal

Table 2 Summary of microchemical and microstructural examinations

Alloy	He (appm)	Dose (dpa)	Temp (°C)	Cr bf (wt%)	Cr af (wt%)	Segr. Ratio (%)	Ni bf (wt%)	Ni af (wt%)	Segr. Ratio (%)	Cavity density (/nm ³)	Cavity Size (nm)	Swelling (%)
SUS304	0	1	300	18.2	14.4	-20.9	8.7	15.4	77.0	-	-	-
	15	1	300	18.2	10.7	-41.2	8.7	16.8	93.1	5.21×10 ⁻⁶	4.9	0.03
	2000	1	300	18.2	11.3	-37.9	8.7	16.5	89.7	1.37×10 ⁻⁵	4.7	0.07
SUS347	15	1	300	17.6	11.6	-34.1	10.01	18.5	83.2	1.76×10 ⁻⁶	4.8	0.01
SUS310	15	1	300	25.5	14.6	-42.7	20.42	38.77	89.9	2.82×10 ⁻⁶	5.2	0.02
XM19	0	1	300	21.9	10.6	-51.6	11.9	29.4	147.1	1.37×10 ⁻⁶	8.5	0.04
	15	1	300	21.9	6.7	-69.4	11.9	41.2	246.2	1.42×10 ⁻⁶	10.3	0.72
	2000	1	300	21.9	9.1	-58.4	11.9	33.8	184.0	3.50×10 ⁻⁶	3.5	0.06

bf:before, af:after, Segr.Ratio:Segregation Ratio

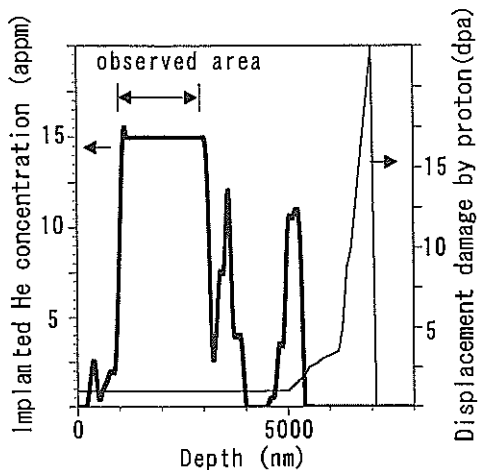


Fig.1 Depth distribution of displacement damage and preinjected Helium concentration simulated by TRIM

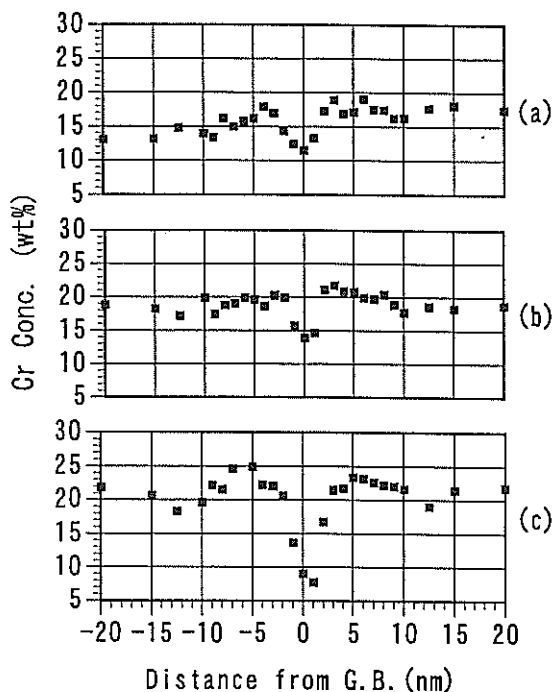
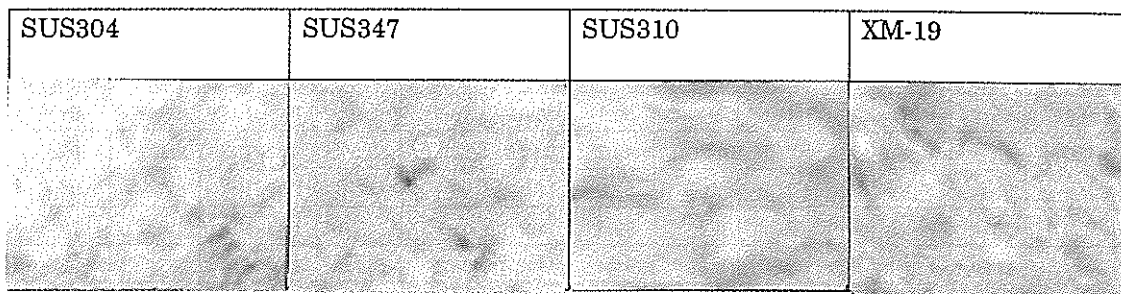
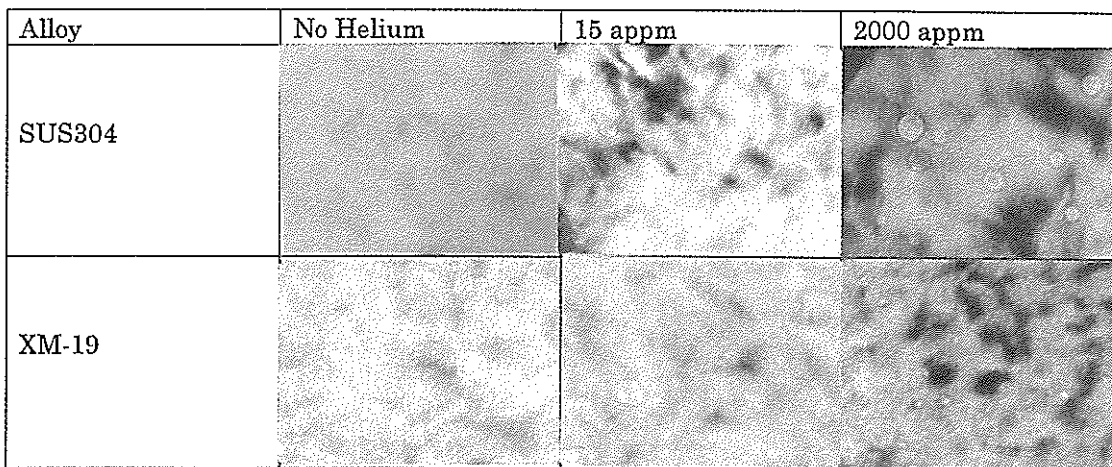


Fig.2 Cr concentration near grain boundaries in irradiated specimens. (a) SUS 304, (b)SUS 347and (c)XM-19



(A)



(B)

20nm

Fig3 Microstructures of specimens after irradiation.

(Dose : 1dpa, Temp.:300°C, Helium concentration (A) 15appm (B) 0-2000appm)

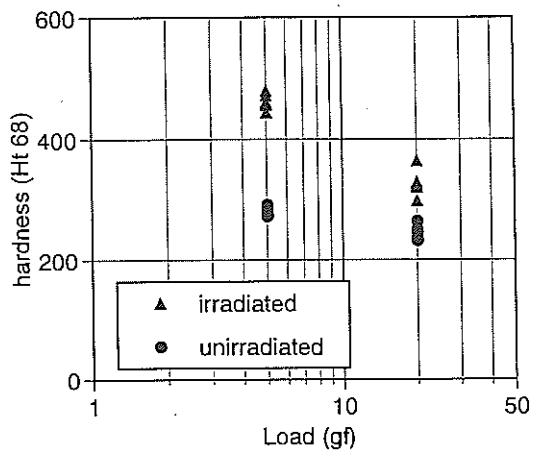


Fig4 Result of micro-indentation test.
 (XM-19 Dose:1 dpa,Temp.:300°C, He
 concentration 15appm)